[Type text]

1   **Short title:** The role of *RGO* in plant development

2   **Corresponding author:** Jas Singh

3

4   **Title:** The Arabidopsis gene *RGO* mediates cytokinin responses and increases seed yield

5

6   Jhadeswar Murmu[1], Ghislaine Allard[2], Denise Chabot[1], Eiji Nambara[3], Raju Datla[4], Shelley

7   Hepworth[5], Rajagopal Subramaniam[1], and Jas Singh[1]

8

9   [1]Ottawa Research and Development Centre, Agriculture and Agri-Food Canada, Ottawa, Ontario,

10   K1A 0C6, Canada

11   [2]Public Health Agency of Canada, Ottawa, Ontario, K1A 0K9, Canada

12   [3]Department of Cell and Systems Biology, University of Toronto, Toronto, Ontario M5S 3B2,

13   Canada

14   [4]Global Institute for Food Security, 110 Gymnasium Place Saskatoon, SK S7N 0W9

15   [5]Department of Biology and Institute of Biochemistry, Carleton University, Ottawa, Ontario, K1S

16   5B6, Canada

17

18   **One-sentence summary:** *RGO,* a novel gene from Arabidopsis, is essential for plant development,

19   mediates CK signaling and increases seed yield in Arabidopsis and rapeseed when overexpressed.

20   **Author contributions:** JM and JS designed the experiments; JM, GA, and DC performed the

21   experiments; EJ quantified cytokinins; JM, JS and RS analyzed the data, and JM, RD, SRH, RS,

22   JS wrote the manuscript. RS and JS contributed equally to this research. JS agrees to serve as author

23   responsible for contact and ensures communication.

27

[Type text]

1 Abstract

2 A novel gene, *At1g77960*, from *Arabidopsis thaliana* was characterized. *At1g77960* transcripts
3 accumulate to very high levels in plants ectopically overexpressing the *Golden2-like1* (*GLK1*)
4 transcription factor and is designated as a <u>Response to GLK1 Overexpression</u> (*RGO*) gene. *RGO*
5 encodes a protein with domains of tandem QH and QN repeats. Transcripts and promoter GUS
6 reporter analyses indicated that *RGO* is expressed in roots, leaves, stems, floral and siliques tissues
7 but not in seeds. Expression of the RGO:YFP fusion protein demonstrated that *RGO* is localized
8 to the endoplasmic reticulum. MicroRNA mediated silencing of *RGO* resulted in severe reductions
9 in vegetative and root growth, delayed flowering and reduced seed yield and viability, suggesting
10 that *RGO* is essential for plant development. Conversely, ectopic overexpression of *RGO* resulted
11 in enhanced vegetative growth including increased axillary bud formation and a 20% higher seed
12 yield. Stable overexpression of *RGO* in *Brassica napus* also produced a similar increase in seed
13 yield. Cytokinin (CK) response assays including root growth, green calli formation from excised
14 hypocotyls and chlorophyll retention during dark-induced senescence suggest that one role of *RGO*
15 is to mediate CK responses in plant development. These results suggest that *RGO* could be a target
16 gene for increasing crop seed yields.

17 Keywords

19

[Type text]

Introduction

1   Significant progress have been made in our understanding of the role of cytokinins (CK) in plant

2   growth, and development. Through interactions with other hormonal pathways and transcriptional

3   factors, CKs plays an important role in a variety of plant processes including greening (Cortleven

4   and Schmülling, 2015), etioplast-to-chloroplast transition (Cortleven et al., 2016), root greening

5   (Kobayashi et al., 2012; 2017), shoot and shoot development (Howell et al., 2003; Kieber and

6   Schaller, 2014; Raines et al., 2016) and delay in leaf senescence (Gan and Amasino, 1995; Kim et

7   al., 2006; Kieber and Schaller, 2014; Raines et al., 2016; Talla et al., 2016). The current knowledge

8   of CK signalling involves a multistep signal transduction system that begins with the perception of

9   CK by the Arabidopsis Histidine Kinases (*AHK2*, *AHK3*, *CRE1*/*AHK4*) in the endoplasmic

10   reticulum (ER) phosphate transfer via the Arabidopsis Histidine Phosphotransfer proteins (AHPs).

11   The information is transmitted to the nucleus where the transcription factors such as the type-B

12   Arabidopsis Response Regulators (ARRs) affect gene expression (Kieber and Schaller, 2014;

13   Romanov et al., 2018).

14   The roles of CK in chloroplast development are mediated by core components of the CK signalling

15   pathway which includes the CK receptors *AHK2* and *AHK3* and the response regulators *ARR1*,

16   *ARR10* and *ARR12* (Cortleven and Schmülling, 2015). Chloroplast development and maintenance

17   in leaves also requires functional *Golden2-like* (*GLKs*) transcription factors (Fitter et al., 2002;

18   Yasumura et al., 2005; Waters et al., 2008; Waters et al., 2009) which are members of the Myb

19   superfamily of transcription factors containing a DNA binding "GARP" domain named after the

20   maize <u>G</u>olden2, the type-B <u>A</u>rabidopsis <u>R</u>esponse <u>R</u>egulators (*ARR*), and the Chlamydomonas

21   <u>P</u>hosphate <u>s</u>tarvation <u>r</u>esponse (*PSR1*) transcription factors (Reichmann et al., 2000). In

22   Arabidopsis leaves, *GLK1* and *GLK2* operate in redundant fashion as only the *glk1 glk2* double

23   mutant showed impaired chloroplast development to display a distinct pale green phenotype (Fitter

24   et al., 2002). The role of *GLK*s in chloroplast maintenance is also linked to leaf senescence,

25   underscored by the observation that elevated expression of the transcription factor *ORE1* triggered

26   early senescence in Arabidopsis through down regulation of *GLKs* and it has been observed that

27   overexpression of *GLK1* delays leaf senescence (Rauf et al., 2013; Garapati et al., 2015). The role

28   of *GLKs* in leaf senescence is also reflected in the observation that overexpression of *GLK1*

29   resulted in the reduction of infection of the necrotrophic pathogen *Botrytis cinerea* (Murmu et al.,

30   2014) as it is known that delay of senescence is a key factor in resistance to this pathogen

31   (Swartzberg et al., 2008; Lai et al., 2011; Wang et al., 2013; Haffner et al., 2015).

[Type text]

1

2 A direct link between *GLKs* and CK signalling however, is lacking. There is evidence to suggest

3 that type B *ARRs* coordinate the expression of *HY5* (elongated hypocotyl 5), which is required by

4 *GLK2* for maximal (although not essential) greening in roots (Kobayashi et al., 2012).

5 Overexpression of *GLK2*, *GNC (GATA, NITRATE-INDUCIBLE, CARBON-METABOLISM-*

6 *INVOLVED*) and *CGA1* (*CYTOKININ-RESPONSIVE GATA 1/GNC-LIKE)* result in root greening,

7 however, neither *GLK1* nor *GLK2* are required for the CK-dependent root greening phenotype

8 (Kobayashi et al., 2012). In tomato, overexpression of *GLK2* in the fruit leads to enhanced CK

9 responsiveness and delayed ripening, thus differentiating function between the two *GLKs* in

10 development programs such as fruit ripening (Lupi et al., 2019). However, the role of *GLKs* in CK

11 response is lacking in leaves. There is no evidence to suggest that *GLKs* can participate in the

12 phosphor-relay step and in this regard, are similar to the CK response regulator *ARR21C*, a

13 truncated form of *ARR21* where the phosphor-relay N-terminus domain is removed (Kiba et al.,

14 2005). Ectopic overexpression of *ARR21C* resulted in altered CK signalling, affecting plant

15 development. *ARR21* has been shown to function in CK signalling as it can complement *arr1* and

16 *arr12* mutants, although its precise role in CK signalling remains to be established (Hill et al.,

17 2013). With the loss of the phospho-regulatory domain, ectopic overexpression of *ARR21C* in

18 Arabidopsis produced a range of highly abnormal phenotypes with hypersensitivity to exogenous

19 applications of very low levels of CK (Tajima et al., 2004; Kiba et al., 2005). To explore if an

20 association exists between *GLK1* overexpression and CK signalling, we focussed on a previously

21 uncharacterized Arabidopsis gene *At1g77960*, which was highly upregulated by ectopic

22 overexpression of *GLK1* (Savitch et al., 2007). An examination of the microarray data from CK

23 hypersensitive plants overexpressing *ARR21C* (Goda et al., 2008) also indicated that this gene was

24 also substantially overexpressed.

25 Few other studies have implicated *At1g77960* in different plant processes. The *At1g77960* gene

26 transcripts was upregulated in the *esr1-1* (enhanced stress response 1) mutant with increased

27 resistance to the fungal pathogen *Fusarium oxysporum* (Thatcher et al., 2015) and was

28 downregulated after infection with the bacterial pathogen *Pseudomonas syringae* pv tomato

29 Dc3000 (Lewis et al., 2015). Despite the correlation between levels of gene expression in various

30 plant processes, detailed characterization of *At1g77960* is lacking. Therefore, in this study we

31 designated *At1g77960* gene as *Response to GLK1 Overexpression (RGO)*, and investigated its

[Type text]

1   potential role in modulation of CK response and its significance in plant development,
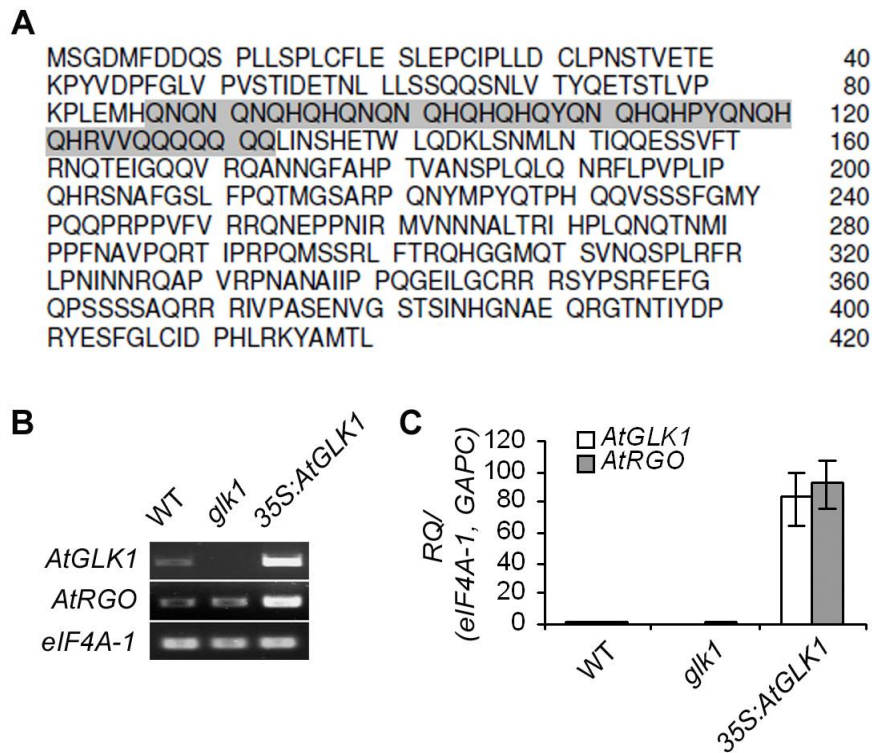
2   performance and seed yields.

3

4   **Results**

5   **Arabidopsis *RGO* is a novel gene discovered from ectopic overexpression of *GLK1***

6

7   Transcripts of *AtRGO* were observed to be highly accumulated in Arabidopsis plants ectopically

8   overexpressing *GLK1* (Savitch et al.*,* 2007). A detailed RT-PCR and qPCR analyses demonstrated

9   that *RGO* transcripts are highly upregulated in plants constitutively overexpressing *GLK1* (Fig. 1,

10 B and C). Transcript levels in the *glk1* mutant remained unchanged when compared to the WT

11 (Fig. 1, B and C) suggesting that *RGO* is not directly regulated by *GLK1*. An examination of the

12 microarray data from CK hypersensitive plants overexpressing *ARR21C* also upregulated *RGO*

13 transcripts by nine fold (Supplementary Table. S1). To further substantiate the observation of

14 *GLK1* in the activation of *RGO* overexpression, we cloned and overexpressed *TaGLK1* from bread

15 wheat (NCBI Accession EF105406) in Arabidopsis. Arabidopsis plants overexpressing *TaGLK1*

16 also showed a high upregulation of *RGO* (Supplemental Fig. S1). *RGO* is a single copy gene

17 encoding a 48 kilo Dalton (kDa) glutamine (Q) rich (14%) protein of 420 amino acids. The N-

18 terminus of the deduced protein contains a hydrophobic region (45% hydrophobic residues)

19 followed by tandem repeats of Q with either asparagine (Q/N) or histidine (Q/H) followed by a 7

20 amino acid Q repeat (Fig. 1A). QQ repeats are also observed throughout the RGO protein sequence.

21 *RGO* has been erroneously annotated as repressor *ROX1-like* in TAIR (The Arabidopsis

22 Information Resource) database; *ROX1* encodes a DNA-binding protein that represses the

23 expression of hypoxia genes in yeast (Balasubramanian et al., 1993; Deckert et al., 1995). Protein

24 sequence alignments between *RGO* and the yeast repressor ROX1 showed no homology. As well,

25 RGO does not contain a high-mobility group (HMG) DNA binding domain that is characteristic of

26 repressor ROX1 proteins. Similarly, several genes with deduced protein sequence homology to

27 RGO in *Camelina sativa*, *Brassica rapa* and *Brassica napus* (Supplemental Fig. S2) have also been

28 incorrectly annotated as repressor ROX1 proteins. Proteins with homology to RGO have yet to be

29 identified in the sequence databases of plants outside of the *Cruciferae* species.

[Type text]

A

```
MSGDMFDDQS PLLSPLCFLE SLEPCIPLLD CLPNSTVETE      40
KPYVDPFGLV PVSTIDETNL LLSSQQSNLV TYQETSTLVP      80
KPLEMHQNQN QNQHQHQNQH QHQHQHQYQN QHQHPYQNQH     120
QHRVVQQQQQ QQLINSHETW LQDKLSNMLN TIQQESSVFT     160
RNQTEIGQQV RQANNGFAHP TVANSPLQLQ NRFLPVPLIP     200
QHRSNAFGSL FPQTMGSARP QNYMPYQTPH QQVSSSFGMY     240
PQQPRPPVFV RRQNEPPNIR MVNNNALTRI HPLQNQTNMI     280
PPFNAVPQRT IPRPQMSSRL FTRQHGGMQT SVNQSPLRFR     320
LPNINNRQAP VRPNANAIIP PQGEILGCRR RSYPSRFEFG     360
QPSSSSAQRR RIVPASENVG STSINHGNAE QRGTNTIYDP     400
RYESFGLCID PHLRKYAMTL                           420
```

B   **C**

Figure 1

Deduced amino acid sequence and upregulation of *Arabidopsis Response to GLK1 Overexpression* (*RGO*, *At1g77960*). (A) amino acid sequence of *At*RGO in single-letter code and the glutamine rich region is highlighted in gray. Numbering of amino acids are on the right. (B) Transcripts accumulation of *AtGLK1* and *AtRGO* in wild-type (WT), *glk1* mutant, and 35S:*AtGLK1* plants with RT-PCR compared to *eIF4A-1*, a housekeeping gene transcripts; (C) *AtGLK1* and *AtRGO* transcripts with qPCR relative to *eIF4A-1* and *GAPC,* two housekeeping gene transcripts. Relative transcripts represent as mean fold change values ± standard error of mean (SEM) from three biological replicates.

***RGO* expression is ubiquitous in Arabidopsis vegetative and floral tissues**

RGO transcripts were expressed ubiquitously in Arabidopsis plant tissues such as roots, leaves,

stem and internodes, inflorescence apex, and siliques as demonstrated by semi-quantitative RT-

PCR (Fig. 2A). *RGO* transcripts were relatively abundant in cauline leaves and scarce in mature

siliques as validated by qPCR experiments (Fig. 2B). We also generated transgenic lines

expressing a 1.9 kb *RGO* promoter fragment fused to GUS reporter gene in the WT (Col-0)

background to localize expression of this gene. Gus expression was most intense in early seed

germination, starting one day after germination, and in cotyledons and slowly progressed to

[Type text]

1   vascular tissues in the root (Fig. 2C). In later stages of plant development, expressions were

2   mainly confined to veins of rosette and cauline leaves. In inflorescence tissues, expressions were

3   prominent in the stem, young apex, and young siliques. By contrast, both mature flowers and

4   mature siliques displayed reduced GUS accumulation and no expression was detected in seeds.

5   The *RGO* expression is also diurnally regulated (Supplemental Fig. S3); *RGO* transcripts began

6   to accumulate early in the light cycle and peaked during the middle of the light cycle, then

7   gradually diminished towards the end of the light-cycle and remain unchanged during the dark

8   cycle (Supplemental Fig. S3). This data suggest that *RGO* expression is light or photoperiod

9   sensitive.

10
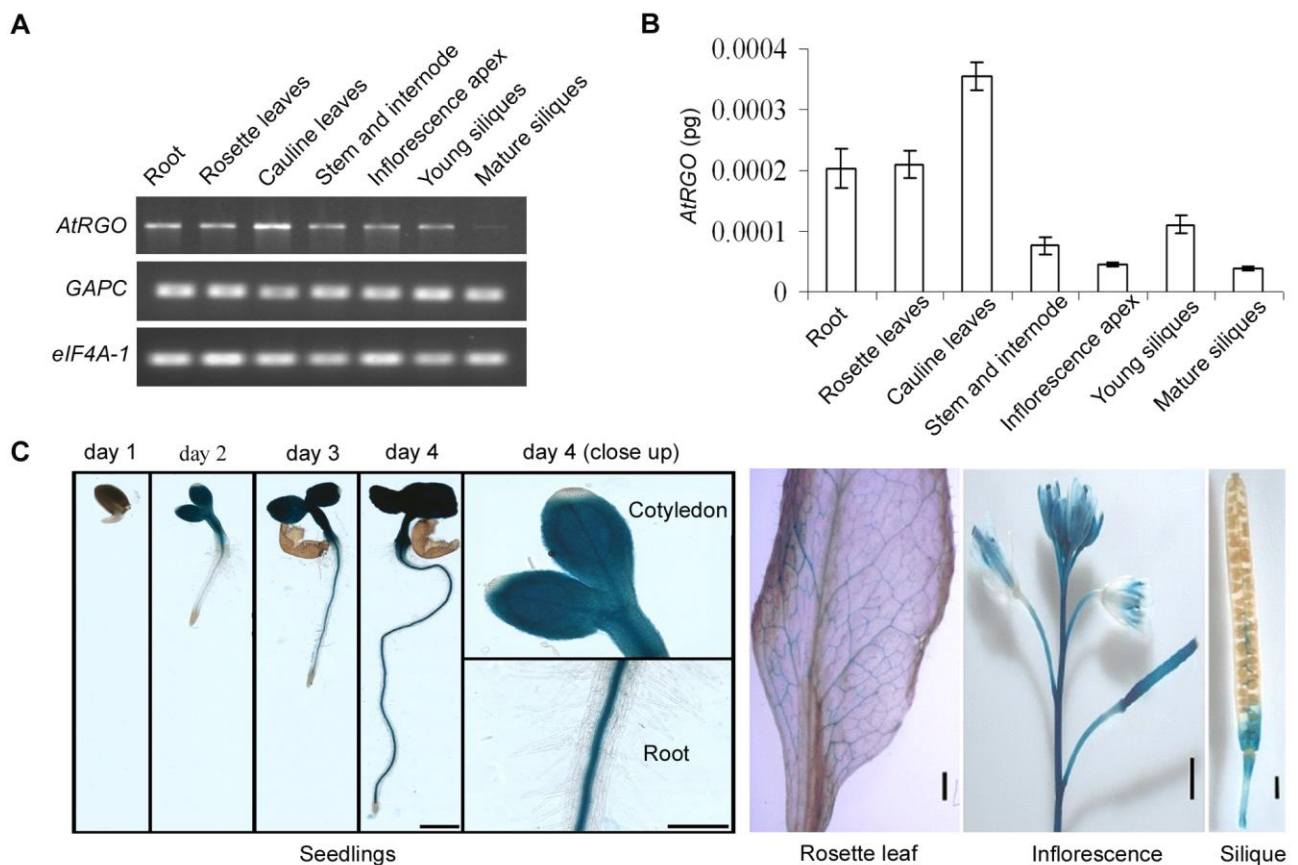
11

12

13

14   **Figure 2**

15   **Expression pattern of *AtRGO*.** (A) *AtRGO* transcripts accumulation in wild-type (WT) Col-0

16   with RT-PCR compared to *eIF4A-1* and *GAPC*, two housekeeping control transcripts; (B)

[Type text]

1 Absolute quantification of *AtRGO* transcripts with qPCR. Transcripts represented are mean fold
2 change values ± standard error of mean (SEM) from three biological replicates; (C) *AtRGO*
3 promoter driven reporter GUS reporter gene expression in WT plants. GUS expression was
4 observed starting one day after germination; GUS expression was intense in cotyledons and
5 slowly progressed to vascular tissues in the root. Scale bar, 200 □m in seedlings, and bar, 1 cm in
6 mature tissues.
7
8

9 **RGO is localized to the Endoplasmic Reticulum**

10 The presence of hydrophobic amino acid residues at the N-terminus of the RGO protein suggested

11 that it is most likely membrane localized. As the RGO protein sequence did not reveal any

12 functional domains and organelle localization signals, we undertook cellular localization studies

13 to provide insights into the potential function of RGO. A C-terminal translational fusion of *RGO*

14 with YFP (yellow fluorescent protein) under the control of the Cauliflower Mosaic virus (CaMV)

15 35S promoter was constructed and stable transgenic Arabidopsis plants were generated. Transgenic

16 plants expressing 35S:YFP were used as a control. As displayed, free YFP fluorescence were

17 observed to be evenly distributed in the cytoplasm and nucleus of leaves of 35S:YFP transgenic

18 plants, (arrows, Fig. 3, A and C). The nuclei were identified by DAPI staining in Fig. 7B. In

19 epidermal cells of leaves expressing 35S:*RGO:*YFP, YFP fluorescence was observed in distinct

20 locations in the cytoplasm and surrounding the nucleus (Fig. 3, D and F). Unlike the control

21 35S:YFP leaf tissues, no fluorescence was detected in the nucleus (Fig. 3F). The nuclei were

22 identified by DAPI staining in Fig. 7E. This pattern of fluorescence is consistent with proteins

23 localizing to the endoplasmic reticulum (ER) (Nelson et al., 2007; Wulfetange et al., 2011). The

24 presence of the hydrophobic N-terminus of RGO likely enables it to be localized to the membranes.

25 To confirm these findings, FM4-64FX, a plasma membrane specific fluorescent dye was used in

26 combination with YFP fluorescence to demonstrate that 35S:RGO-YFP fluorescence (yellow) was

27 distinctly separated from the FM4-64FX (blue) plasma membrane stain (Fig. 3H), whereas, free

28 fluorescence in the control leaf tissues (35S:YFP) overlapped (white colour) with the plasma

29 membrane as well as the nucleus (Fig. 3G). These fluorescence patterns were indicative of ER

30 localization and suggest that RGO is associated with the ER and not the plasma membrane. To

31 further confirm the ER localization of RGO protein, we compared transient overexpression of an

32 ER marker, 35S:GFP-HDEL (Batoko et al., 2000) to the expression of 35S:RGO-YFP in tobacco

33 leaves. The expression pattern of RGO (Fig. 3I) is identical to the ER expression pattern of

34 35S:GFP-HDEL (Fig. 3J) and confirms that RGO is localized to the ER.

8

[Type text]
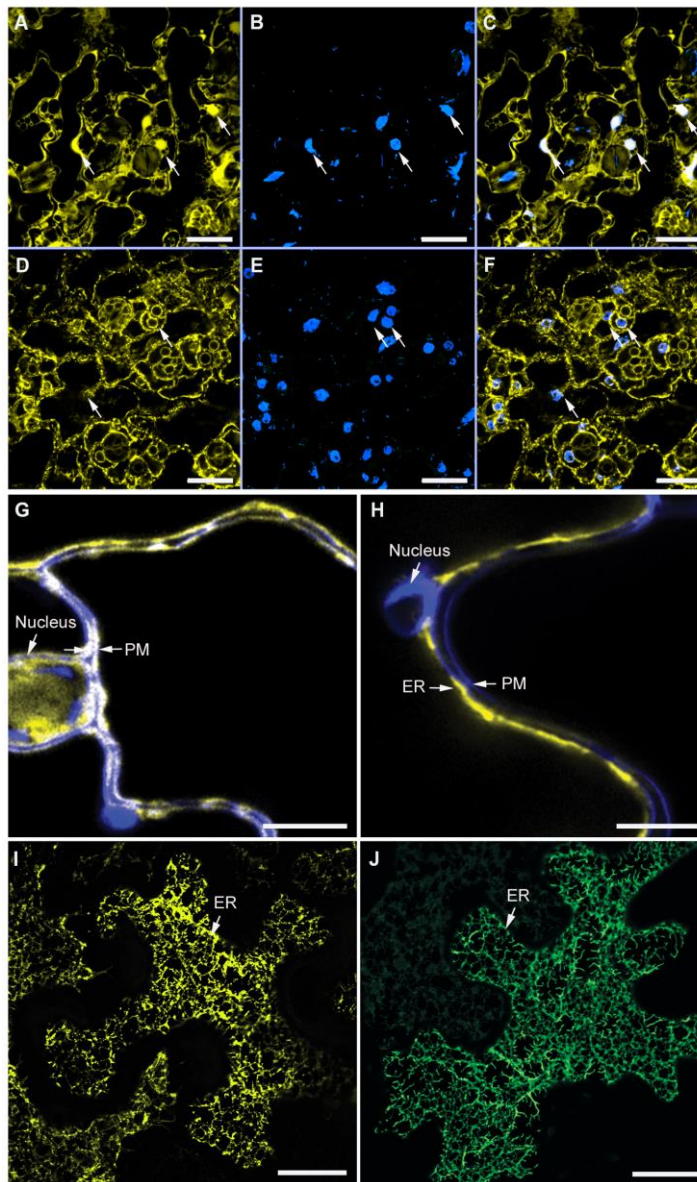
Fig. 3

Subcellular localization of *At*RGO-YFP fusion protein by confocal microscopy in transgenic Arabidopsis leaves and tobacco leaves. Plants expressing 35S:YFP were used as positive control (A-C) for comparing *At*RGO-YFP fusion expression (D-F). (A and D), YFP signal in yellow; (B and E), DAPI strained nuclei in blue; (C and F) merged. Arrow head shows the nucleus and endoplasmic reticulum (ER). Zoom in view of 35S:YFP (G) and *At*RGO:YFP (H) with FM4-64FX stain. YFP fluorescence in yellow and plasma membrane stain in blue, a false colour for contrast is shown in G-H and arrow head shows the nucleus and plasma membrane (PM) in G-H. Transient expression of *At*RGO-YFP (I) and GFP:HDEL, an ER marker (J) in tobacco leaves. Arrow head shows the ER in I-J. Scale bar, 20 μm in A-F and 5 μm in G-J.

9

[Type text]

1   *RGO* **is required for root development, normal growth and flowering**

2   Phenotypic studies were undertaken to further elucidate the function of *RGO*. We obtained three

3   T-DNA insertion lines (Salk_025545, Salk_109614, and Salk_109424) for *RGO* from the

4   Arabidopsis Biological Resource Center (ABRC), Ohio State University, USA. Arabidopsis T-

5   DNA design tool (http://signal.salk.edu/tdnaprimers.2.html) indicated that Salk-109424 has a

6   second T-DNA insertion in gene *At5g33175*. We could not detect T-DNA insertions in the *RGO*

7   gene in the Salk_109424 line (data not shown). However, we identified a T-DNA insertion in the

8   first exon of *RGO* at 33 bp down stream of the transcription start site in the Salk_109614 plants

9   (Supplemental Fig. S4A). Similarly, we identified a T-DNA insertion in Salk_025545 in the fifth

10   intron at 1170 bp down stream of transcription start site (Supplemental Fig. S4A). Both

11   Salk_109614 and Salk_025545 T-DNA insertion lines produced uninterrupted full length *RGO*

12   transcripts (Supplemental Fig. S4D), which was verified by sequencing the *RGO* gene transcripts

13   from both Salk_109614 and Salk_109424 plants and showed that the transcripts were identical to

14   the WT.

15   As we could not isolate homozygous T-DNA insertional knockout lines for *RGO*, we generated

16   artificial micro RNA (amiR) silencing lines for the gene. We screened 72 Basta resistant primary

17   transformed plants and identified two lines (*rgo*-1 and *rgo*-2) and transcripts analyses of T2

18   generations of by RT-PCR as well as qPCR revealed that these two lines had significant reductions

19   in transcript accumulation of *RGO* (Fig. 4 A). Plants from both *rgo* lines exhibited a minimum of

20   two-week delay in bolting compared to the WT (Fig. 4, B and C). These plants were able to set

21   seeds albeit to much lesser degrees than WT plants and with the phenotypes being stable in

22   subsequent generations. Seeds from subsequent generations (T4) showed substantial decreased

23   germination rates (70-80%) compared to the WT (Supplemental Fig. S5A). To validate the

24   phenotypes observed in the *RGO* silenced (*rgo*) lines, we generated Arabidopsis lines that

25   constitutively expressed *RGO* (35S:*RGO*). Section and staining of *rgo* seeds showed impaired

26   embryo development compared to the WT and to the 35S:*RGO* plants. In the *rgo* lines, the majority

27   of embryos were immature, which corroborated with the lethality of seeds and consequently

28   decreases in seed germination. (Supplemental Fig. S5B). In light of these findings that linked *RGO*

29   with plant development in vegetative tissues, we examined the effect of *RGO* silencing on root

30   growth. Compared to the WT seedlings, *rgo* seedlings grew significantly slower and with a 67%

31   decrease in root length compared to the WT, whereas the root length of 35S:*RGO* seedlings were

[Type text]

1 similar to the WT (Fig. 5, A and B). Collectively, these results suggest that *RGO* is required for

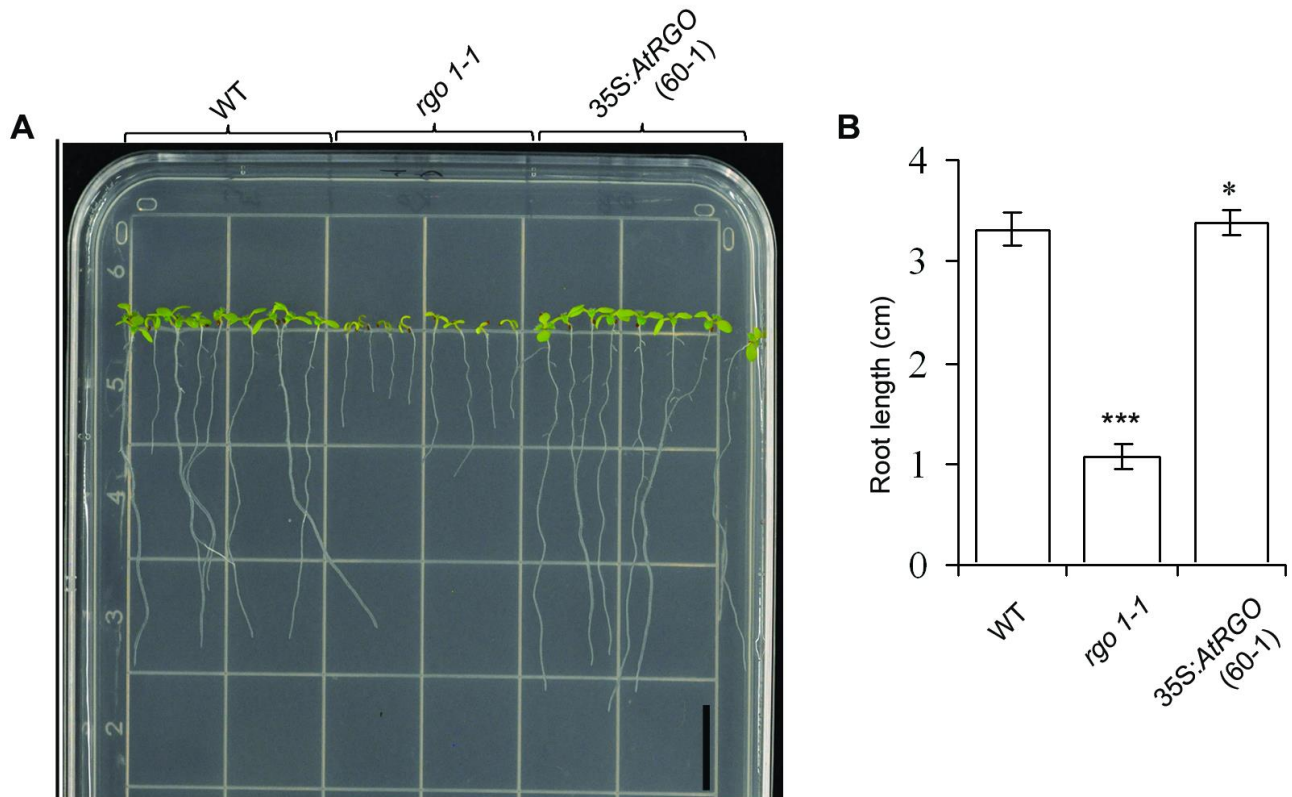2 normal growth as well as viable seed development.

3
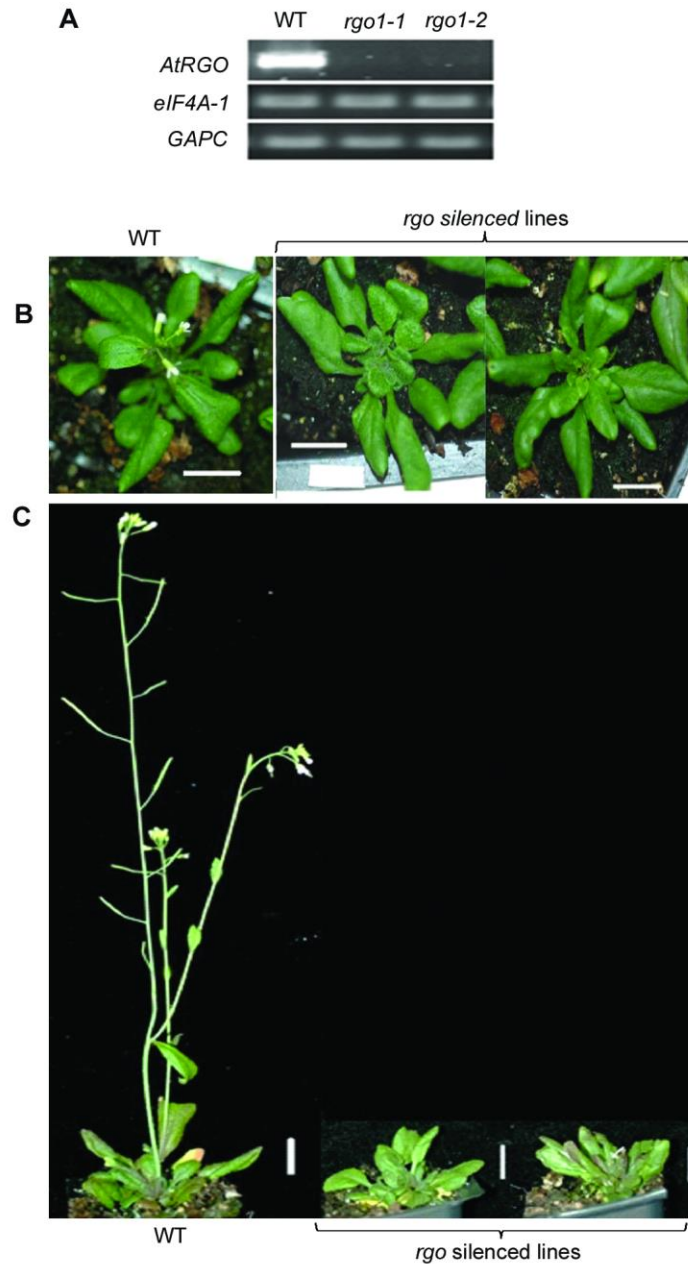
4

5

6 **Figure 4**

7 **Phenotype of *rgo* plants compared to WT (Col-0).** (A) A RT-PCR of full length *AtRGO*

8 transcripts in WT and *rgo* plants compared to *eIF4A-1* and *GAPC* transcripts; (B) qPCR of

9 *AtRGO* transcripts in WT and *rgo* plants; (C) phenotype at four-week age; (D) phenotype at six-

10 week age. Scale bar, 1 cm in C-D.

11

11

[Type text]

1

2

3

4

5

6 **Figure 5**

7 **Root growth phenotype of WT, *rgo* and *35S: AtRGO* lines at seven days post germination.**
8 (A) representative images on minimal media (MM), (B) corresponding root length. Error bar =
9 standard error of mean. Scale bar, 1 cm in A. Statistical significance of root lengths were
10 analyzed using student's t-test: Two sample assuming unequal variance at 95% confidence level.
11 *** represents the p value < 0.00000001, and * represents p value > 0.1.

12

13 **Constitutive expression of *RGO* increases growth and seed yield**
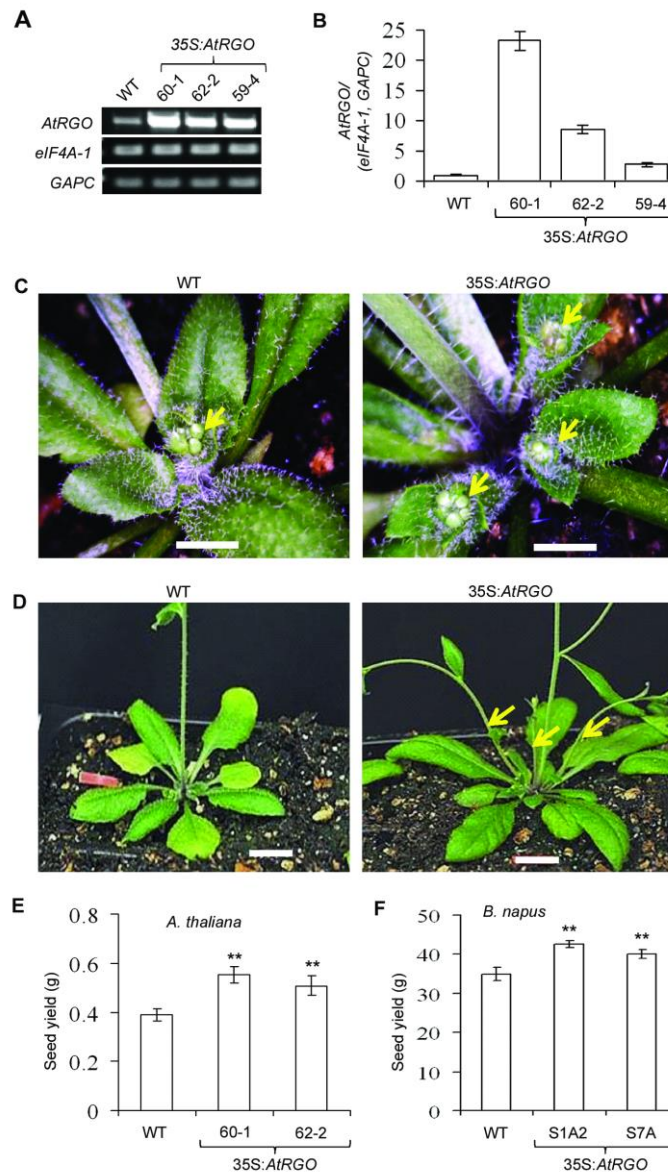
14

15 Analyses of T3 generations of three independent 35S:*RGO* lines indicated a significant

16 accumulation of *RGO* transcripts, with line 60-1 exhibiting a 20-fold increase in transcript

17 accumulation compared to the WT (Fig. 6, A and B). All the lines overexpressing *RGO* showed an

18 acceleration of flowering by one-week, when compared to the WT under long-day growth

19 conditions (Fig. 6C). Additionally, aerial vegetative growth were observed 2-3 weeks earlier

[Type text]

1   compared to the WT and by week four, the transgenic plants showed increased numbers of axillary

2   vegetative buds per rosette compared to the WT resulting in increased number of shoots per rosette

3   (Fig. 6D). We also observed that the length of the rosette leaves in *RGO* transgenic plants were

4   considerably longer than that of the WT (Supplemental Fig. S6). Given the significant increase in

5   biomass and shoots, we assessed seed yield in these transgenic plants overexpressing *RGO*. On

6   average, there was a 20 % higher seed yield than the WT under identical growth conditions (Fig.

7   6E). We were interested to know if the seed yield phenotype can be recapitulated in related Brassica

8   species. We generated two lines of *Brassica napus* overexpressing *AtRGO* (35S:*RGO*:). Stable

9   transgenic *B. napus* (T3) lines overexpressing *RGO* showed similar increased vegetative branching

10   compared to the WT (Supplemental Fig. S7) with an average 18 % increase in seed yields (Fig.

11   6F) when grown under controlled environmental conditions.

[Type text]

Figure 6

Phenotype of *35S:AtRGO* plants compared to WT. (A) A RT-PCR of full length *AtRGO* transcripts compared to *eIF4A-1* and *GAPC* transcripts in WT and three independent lines of *35S:AtRGO* plants; (B) qPCR of *AtRGO* transcripts in WT and *AtRGO* overexpressing lines; (C) Four-week old plants; (D) Five-week old plants. Emergence of inflorescence buds are shown with arrow head in C and axillary buds in D; (E) Average seed yield from 10 Arabidopsis plants of WT and *35S:AtRGO* from a long-day photoperiod growth conditions; (F) seed yield from individual plants of *B. napus* in WT and *35S:AtRGO* (two lines). Scale bar, 1cm in C-D. Statistical significance was analysed using student's t-test: Two-sample assuming unequal variances at 95% confidence level compared with empty vector. The p value for each analysis is shown as asterisk, where p value ≤ 0.001 (**). Error bar = standard error of mean.

14

[Type text]

1 ***RGO* mediates CK responses to regulate endogenous CK levels and safeguard the positive**

2 **effects of CK in plant development**

3

4 To explore if a relationship exists between *GLK1* overexpression, *RGO* upregulation and CK

5 responsiveness, we first examined if ectopic overexpression of *GLK1* has an effect on sensitivity

6 to CK signalling using the green calli/shoot regeneration assay (Kiba et al., 2004). Robust green

7 calli formation was observed for external application of 0.005 µM BA for *GLK1* overexpressing

8 plants compared to 0.1 µM BA for the WT (Fig.7A). This observation prompted us to use *RGO*

9 silencing and overexpression to determine if RGO can, in part, be a factor in CK response. One of

10 the well-documented effects of exogenous CK on plants is shortened root growth (Skoog and

11 Miller, 1957) and that CK levels regulate root development (Werner et al., 2001; Werner and

12 Schmülling, 2009). As observed, *rgo* lines display shorter root growth compared to the WT and

13 *RGO* overexpressor seedlings (Fig. 5A). Therefore, we compared the root growths of the WT,

14 *35S:AtRGO* and *rgo* seedlings in the presence of 5 μm Zeatin, a synthetic CK. The effect on root

15 growth inhibition by Zeatin was partially mitigated in *RGO* overexpressing seedlings compared to

16 the WT and *rgo* seedlings suggesting that overexpression of *RGO* can potentially dampen the

17 inhibitory effects of CK on root development (Fig. 7B). In addition to the effects on root growth,

18 it is known that external applications of CK also facilitate green calli and shoot regeneration. Green

19 calli formation from excised hypocotyl was evaluated to measure CK responses (Kiba et al., 2005).

20 The results showed that while the *RGO* overexpressing and WT plants showed minimal differences

21 in their response to exogenous applications of BA, the *rgo* plants were unable to respond to BA

22 and did not induce green calli formation (Fig. 7B). External applications of CK has also been shown

23 to improve chlorophyll retention and delay dark-induced senescence in leaves (Gan and Amasino

24 1995; Kim et al 2006; Talla et al 2016). As well, increased endogenous levels of CKs have been

25 shown to be able to delay senescence in plants (Richmond and Lang, 1957; Lin et al., 2002; Ma

26 and Liu, 2009; Zhang et al., 2010; Liu et al., 2012). We assessed chlorophyll retention in detached

27 leaves after dark-induced senescence in the absence or presence of BA. After seven days of dark

28 incubation in the absence of BA (7d-BA), neither the WT nor the *rgo* plants retained any

29 chlorophyll (Chl) (Fig. 7D). In contrast, 35S:*AtRGO* leaves retained 26% of the Chl content (Fig.

30 7D). In the presence of BA (7d +BA), 35S:*AtRGO* plants did not lose any Chl (Fig. 7D).

31 Interestingly, in the 7d+BA treatment, the *rgo1-1* silenced line also retained significantly more Chl

32 than the WT (Fig. 7D). This retention could result from increased CK accumulation in the silenced

15

[Type text]

1 line facilitating some signalling even though *RGO* is knocked down. Analyses of bioactive CK

2 levels confirmed that that both trans-zeatin (tZ) and 2-isopentenyladenine (2iP) were significantly

3 elevated in the *rgo* plants compared to the WT (Fig. 7E). There was a modest but significant

4 decrease in 2iP levels in *RGO* overexpressing plants (Fig. 7E). This increase in endogenous CK

5 levels in *rgo* plants (Fig. 7E) is reflected in lower transcript levels encoding CK degrading enzymes

6 CK oxidases *CKX4* and *5*, (Fig. 7F). Taken together, these results suggest that *RGO* can respond

7 to modulate CK levels in a fashion that facilitates or promotes favorable plant processes. It can

8 attenuate the negative effect of external CK application on root growth and conversely, positively

9 facilitate CK induced delay of senescence in excised leaves.

10

11

16
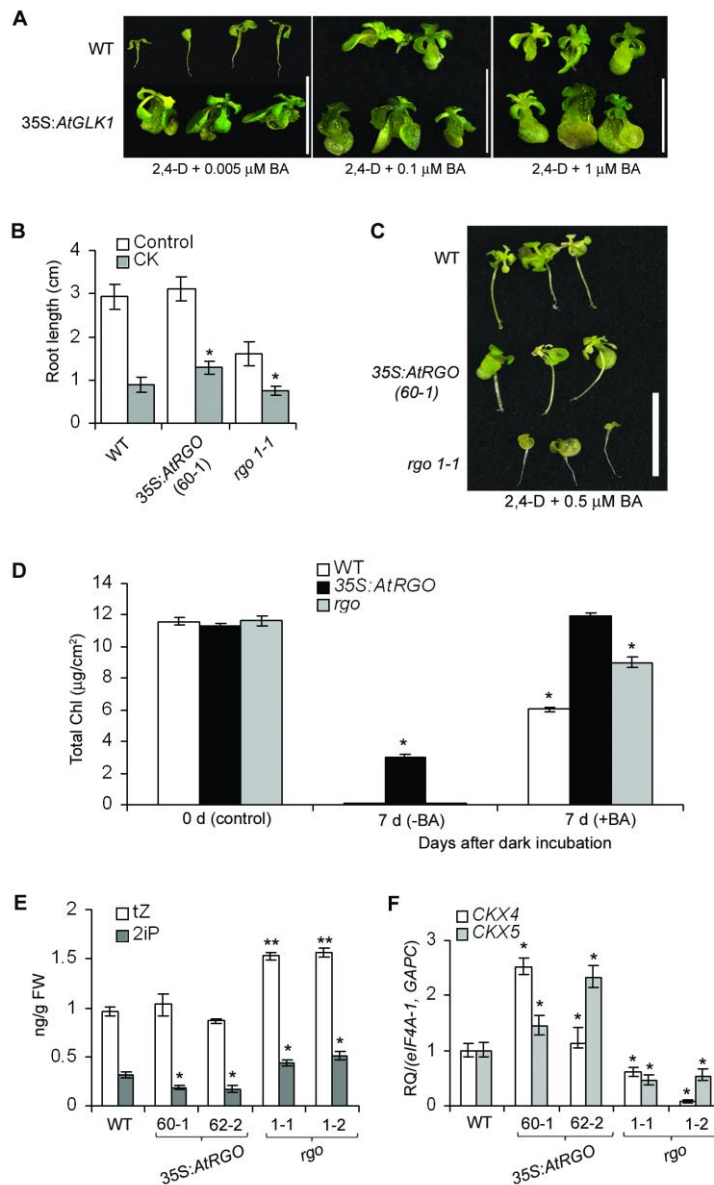
[Type text]

1 **Figure 7**
2 **Cytokinin (CK) response, CK levels in 35S:*AtRGO* and *rgo* silenced plants.** (A)
3 Hypersensitive response of *35S:AtGLK1* plants to BA, a synthetic cytokinin (CK), in green calli
4 formation. WT and *35S:AtGLK1* seeds were germinated in dark for five days on half strength MS
5 agar plates then elongated hypocotyls were excised out and grown on half strength MS agar
6 plates supplemented with 0.005 μM 2,4-D plus varying concentration (0.005 to 1 μM) of BA
7 under long-day photoperiod conditions. After 30 days representative callus were photographed.
8 Scale bar = 1 cm. (B) Root length of seedlings at seven days post germination on minimal agar
9 media in absence or presence of 5 μM CK, *represents the p value < 0.001; (C) Green callus
10 formation from excised hypocotyl in presence of 0.005 μM 2,4-D plus 0.5 μM BA (CK) on MS
11 agar plates of WT, 35S:*AtRGO* and *rgo*. Scale bar = 1 cm. (D) Effect of exogenous application of
12 CK on leaf chlorophyll (Chl) retention during dark-induced senescence; (E) Bioactive CK [zeatin
13 (tZ, open bar) and 2-isopentenyladenine (2iP, grey bar)] level in four-week old rosette leaves. p
14 value < 0.001 (**) and p value <0.01 (*). Error bars = SE (n=3). * denotes the significant
15 difference between –BA and +BA treatment (p<0.001, Student's t-test); (F) Relative transcripts
16 of *CKX4* and *CKX5* quantified with qPCR in four week old leaves of wild-type (WT) Col-0,
17 35S:*AtRGO*, and *rgo,* compared to *eIF4A-1* and *GAPC,* two housekeeping control transcripts.
18 Relative transcripts (RQ) represent as mean fold change values ± standard error of mean (SEM)
19 from three biological replicates. Error bars = SE (n=3). * denotes the statistical significant
20 (p<0.001, Student's t-test).
21
22

23 **Discussion**

24

25 *RGO* (*At1g77960*) is a single copy gene in Arabidopsis and encodes a protein of unknown function.
26 *RGO* transcript levels increased highly in Arabidopsis plants ectopically overexpressing either the
27 Arabidopsis *GLK1* or wheat *TaGLK1* transcription factor. *RGO* expression however did not seem
28 to be regulated directly by *GLK1* as *glk1* plants did not show any down regulation of *RGO*. To
29 explore if *RGO* expression was related to requirement for CK levels rather than directly to GLK1
30 overexpression, we measured *GLK1* and *RGO* transcript levels in *atipt1 3 5 7*, a quadruple CK
31 biosynthetic isopentyltransferases mutant severely deficient in endogenous iP- and *t*Z-type
32 cytokinins (Miyawaki et al., 2006). Interestingly, *GLK1* levels were increased over 30-fold in this
33 mutant, but increases in *RGO* levels were not observed (Supplemental Fig.S8). This indicated that
34 increased transcript levels of *RGO* and *GLK1* does not necessarily occur in tandem and suggests
35 that *GLK1* does not directly regulate *RGO*. It is not known why *GLK1* is so highly upregulated in
36 this mutant. It is well established, however, that *GLK1* gene transcription and protein accumulation
37 is regulated by plastid retrograde signals (Martin et al., 2016; Tokumaru et al., 2017) and it is
38 possible to consider that endogenous CK levels may have an effect on this signalling.
39 Nevertheless, this result further underscores the requirement of *RGO* in CK response. The genes

17

[Type text]

1   directly regulating transcription of *RGO* is not yet known. The elucidation of the transcriptional

2   elements directly regulating the expression of *RGO* will have to await identification of binding

3   domains in the promoter region of *RGO* to enable yeast-one-hybrid screens. Unlike *GLK*, *RGO* is

4   not directly involved in the regulation of chloroplast development as *RGO* silenced plants did not

5   show a pale green phenotype (Fig. 4, C and D) observed in the *glk1glk2* plants, which are impaired

6   in chloroplast development (Yasumura et al., 2005; Waters et al., 2008). Moreover, expression of

7   *RGO* (Fig. 3) in all tissue types including photosynthetic tissues also argues against a role critical

8   to chloroplast development. Ectopic overexpression of *RGO* in the pale green *glk1 glk2* background

9   did not rescue chloroplast development, suggesting that it does not act upstream of the *GLKs*

10   (unpublished). More likely, upregulation of *RGO* expression is a response to ectopic

11   overexpression of *GLK1* or type-B ARRs without a phosphor-relay regulatory capacity such as

12   *ARR21C* (Tajima et al., 2004; Kiba et al., 2005) in plants with normal endogenous CK levels.

13

14   **_RGO_ is essential for normal plant development.**

15

16   *RGO* is a single copy gene and the inability to acquire homozygous *RGO* knockout lines without

17   *RGO* transcripts is suggestive that it is essential in plant development. We used amiR silencing as

18   well as ectopic overexpression of *RGO* in Arabidopsis to gain insights into its role in plant

19   development. Observations of reduced transcripts in the *RGO* downregulated (*rgo*) plants were

20   correlated to displays of alterations in normal vegetative and root developments including growth

21   retardation, low seed yields and seed quality leading to lower germination rates in successive

22   generations (Fig. 4, Fig. 5, Supplemental Fig. S5). Conversely, Arabidopsis plants ectopically

23   overexpressing *RGO* consistently produced higher seed yields and vegetative shoots.

24   We hypothesized that at least one explanation for the phenotypes produced by *RGO* overexpression

25   and *RGO* knockdowns could be the result of the modulations of CK response by *RGO*. To this end,

26   we carried out experiments to test specifically whether *RGO* is involved in attenuating or

27   facilitating CK responses. We provide several lines of evidence to support this hypothesis. Firstly,

28   overexpression of *RGO* dampened the effects of external application of CK on root development

29   (Fig. 7A). Conversely, *RGO* silenced (*rgo*) plants showed retarded root growth even in the absence

30   of external CK application (Fig. 5, A and B). Secondly, excised hypocotyls from *RGO* silenced

31   plants were unable to produce green calli/shoot formation in external application of CK (Fig. 7B).

32   Thirdly, increased expression of CK oxidase genes, *CKX4* and *CKX5* in leaves of *RGO*

[Type text]

1 overexpressing plants (Fig. 7E) suggested that one role of the involvement of *RGO* in CK response

2 is to monitor and respond to endogenous levels of CK through *CKX* expression. Elevated CK levels

3 can be attributed to modulation of *CKX* that will prevent the degradation of CKs (Mok and Mok,

4 2001; Werner et al., 2001; 2003). Conversely, knockdown of *RGO* produced significant increases

5 in bioactive CK concomitant with significant decreases of *CKX4* and *CKX5* expression in leaves

6 of the *rgo* plants (Fig. 7D,E). *AtRGO* was identified as a candidate in a GWAS (genome wide

7 association study) study to elucidate genes in shade avoidance

8 (https://explorations.ucdavis.edu/docs/2015/choi.pdf). There was however, no indication the report

9 was peer reviewed and that whether the knockouts of *AtRGO* were genotyped to assure

10 homozygosity as well as absence of *AtRGO* gene transcripts. Nevertheless, it is known that shade

11 avoidance is in part hormonally regulated and involves auxin and cytokinin levels mediated by leaf

12 CKXs (Wu et al., 2017; Yang and Li, 2017). It is conceivable therefore that *AtRGO* could play a

13 role in shade avoidance and should offer opportunities for future studies.

14

15 **Modulation of CK response by *RGO* leads to increased seed yield**

16

17 Ectopic overexpression of *RGO* significantly increased seed yield in both Arabidopsis and *B.*

18 *napus*. It was observed that the Arabidopsis *ckx3 ckx5* double mutant had increased CK levels

19 resulting in increased floral meristems leading to increased seed yield (Bartrina et al., 2011). It is

20 known that tissue specific expression of *CKXs* influence CK levels in those tissues (Mok and Mok,

21 2001; Werner et al., 2001; 2003). Similarly, silencing of *OSCKX2* in rice increased CK

22 accumulation in inflorescence meristems and increased tiller number resulting in enhanced grain

23 yield (Ashikari et al., 2005; Yeh et al., 2015). Grain weight in wheat is also associated with

24 *TaCKX6*-D1, an orthologue of *OSCKX2* (Zhang et al., 2012). Silencing of barley *HvCKX* genes

25 has also been observed to increase seed yield (Zalewiski et al., 2010, 2012, 2014). It is conceivable

26 that increased seed yields in *RGO* overexpressing plants are, in part, a result of enhanced CK

27 signaling. The reduction of *CKX3* and *CKX5* transcript levels in inflorescence buds of *RGO*

28 overexpressing plants (Supplemental Table S4) supports the view that enhanced effects of CK

29 responses are influenced by *RGO*.

30 The mechanism by which *RGO* facilitates CK responses or regulate plant development remains to

31 be elucidated. *RGO* encodes a glutamine (Q) rich protein containing domains of Qs and tandem

32 QNs or QHs. Other than these features, and a hydrophobic N-terminal, RGO contains no known

[Type text]

1   identifiable protein domains. The absence of localization of RGO to the nucleus (Fig. 3) precludes

2   direct functional interactions with transcription factors. Proteins with high QN contents and poly-

3   Q stretches have been associated with neurodegenerative disorders in humans through protein

4   aggregation (Perutz, 1994; Guo et al., 2007; Kuiper et al., 2017) and expansion of Q stretches has

5   been suggested to even modulate the aggregative properties of flanking amino acids (Kuiper et al.,

6   2017). Little is known however of the functional roles of high Q containing proteins in plant

7   development, although Q and HQ domains have been implicated in protein binding/aggregation

8   (Guan et al., 2017) and in RNA binding (Muthuramalingam et al., 2016) in plants. As both poly Q

9   and poly HQ domains are prominent in the RGO protein (Fig. 1A) and as the RGO protein is

10 localized to the ER., we speculate that RGO may interact with CK signaling components as CK

11 signaling components reside in the ER (Caesar et al., 2011; Lomin et al., 2011; Wulfetange et al.,

12 2011; Lomin et al., 2018; Romanov et al., 2018) as well as mediating CK homeostasis by CKXs

13 which takes place in the ER (Schmülling et al., 2003; Werner et al., 2003). Mechanistic aspect of

14 RGO at protein level is under investigation. Identification of transcription factors that directly

15 regulate *RGO* transcription as well as RGO protein/protein interaction partners will aid in

16 elucidation of a mechanism of RGO in plant development.

17 **Materials and Methods**

18 **Plant material**

19

20 For routine propagation of *Arabidopsis thaliana*, seeds from wild-type (Col-0), T-DNA lines (Salk-

21 025545, Salk-109614, Salk-109424), *RGO* silenced lines, 35S:*RGO, glk1* and the *glk1 glk2* double-

22 knockout lines (N9806, N9807, respectively, obtained from the Nottingham Arabidopsis Stock

23 Centre (NASC), Nottingham, UK.), the 35S:*GLK1* and 35S:*TaGLK1* lines were surface sterilized

24 with 2% bleach (v/v) plus 0.001% tween-20, washed five times with sterile water and stratified for

25 two days at 4^0C. Seeds were grown in 48 cell trays on sterilised PRO-MIX MPV potting mixture

26 (Premier Tech Horticulture, Rivière-du-Loup, QC, Canada) and grown in a Conviron PGC 20 CMP

27 model 6050 cabinets (Winnipeg, Manitoba, Canada) at 21-22 ^{0}C, 40-60 % humidity, under long-

28 day conditions (16-h-light/8-h-dark cycle) and a fluorescent light intensity of 100-120 µmol

29 photons $m^{-2} s^{-1}$. Plants were fertilized once a week using 1g per litre solution of 20-20-20 fertilizer

30 (Master Plant-Prod Inc. Brampton, ON, Canada). Similarly, sterilized seeds of *Brassica napus cv*

31 Westar (wild-type) or *RGO* overexpressing transgenic plants were grown in six inch round pots

[Type text]

1   with sterilized mixture of 50% Promix, 25% soil and 25% sand in a Conviron as described above

2   under long-day conditions with a light intensity of 750 µmol photons $m^{-2}\,s^{-1}$. A solution of two

3   grams per litre 20-20-20 fertilizer was given once every third day for the first two weeks and then

4   once a week until seed set. Ten plants each from *Brassica napus* wild-type and two-independent

5   transgenic lines were grown in growth cabinets with identical growth conditions. Seeds were

6   collected from each individual plant and weighed.

7

8   **Promoter GUS construct and analyses**

9

10   A 1.9 kb upstream of the transcription start site ATG of the *At1g77960* gene was PCR amplified

11   with RGO-promo-F and RGO-Promo-R primer pairs using Phusion® High-Fidelity DNA

12   Polymerase (New England Biolabs, Whitby, ON, Canada) with Arabidopsis genomic DNA as the

13   template and was verified by DNA sequencing (Eurofins Genomics, Louisville, KY, USA). The

14   resulting PCR fragment was gel purified and cloned into the gateway entry vector pENTR®/D-

15   TOPO® (Thermo Fisher Scientific, Waltham, MA, USA). The *RGO* promoter: pENTR®/D-TOPO®

16   plasmid was transferred to the binary vector, pMDC162 (Curtis and Grossniklaus, 2003) using LR

17   clonase II (Thermo Fisher Scientific, Waltham, MA, USA) to generate transcriptional fusion with

18   GUS reporter gene. *Agrobacterium tumefaciens* strain GV3101 -pMP90RK containing the *RGO*

19   promoter: pMDC162 plasmid was transformed to Arabidopsis wild-type (Col-0) plants by floral

20   dipping (Clough and Bent, 1998). Primary transgenic plants (T_0) were selected on Murashige and

21   Skoog (MS) basal media plus agar plates in presence of 25 µg ml^{-1} hygromycin. At least 10

22   independent transformed lines from T1 through T3 generation were chosen for GUS analyses.

23   GUS staining was performed as previously described (Murmu et al., 2010). Representative images

24   from three independent lines were presented in figure. All the cloning primers are found in

25   Supplemental Table S2.

26

27   **Constructs for subcellular localization of full length *RGO***

28

29   An overlap extension approach was used to create a C-terminal translational fusion of RGO with

30   YFP. The *RGO* coding sequence (CDS) without the stop codon was PCR amplified from wild-

31   type (WT) leaf cDNA with RGO-cDNA-F plus YFP-RGO cDNA-R primer pairs that generated a

32   1284 bp PCR product with an overlap of 20 bp with the N-terminal of YFP. Next, *YFP* was PCR

[Type text]

1   amplified using RGO-YFP-F plus YFP-R primer pairs that generated a 743 bp PCR product with

2   an overlap of 20 bp at the C-terminal of *RGO* CDS. The above two-PCR fragments were then used

3   as templates for PCR amplification with RGO-cDNA-F plus YFP-R primer pairs to generate a

4   1987 bp *RGO-YFP* translational fusion construct. The resulting PCR product was cloned into the

5   Gateway entry vector pENTR/D-TOPO. Similarly, the YFP CDS was PCR amplified using YFP-

6   F4-Topo plus YFP-R primer pairs and cloned into pENTR/D-TOPO for positive control. All

7   constructs were verified by DNA sequencing. The *RGO-YFP* construct was then transferred to the

8   pK7GW2D binary vector downstream of the Cauliflower Mosaic Virus (CaMV) 35S promoter

9   (35S), using LR clonase II (Thermo Fisher Scientific, Waltham, MA, USA). Similarly, the YFP

10   construct was transferred to the pMDC32 binary vector downstream of the CaMV 35S promoter

11   (Curtis and Grossniklaus, 2003). The resulting 35S:*RGO-YFP*:pK7GW2D and 35S:YFP:pMDC32

12   plasmids were introduced into *Agrobacterium tumefaciens* and were used to transform WT (Col-

13   0) Arabidopsis plants by floral dipping as described in the previous section. Primary transgenic

14   plants were selected on MS agar plates in the presence of 25 μg ml^{-1} hygromycin for the construct

15   in pMDC32 or in the presence of 50 μg ml^{-1} kanamycin for the construct in pK7GW2D.

16

17   **Construction of *RGO* for overexpression studies**

18

19   A full length CDS of *RGO* was PCR amplified from WT leaf cDNA with Xba1- *RGO*-F and Kpn1-

20   *RGO*-R primer pairs. The resulting 1.3 kb DNA fragment was fused to the CaMV 35S promoter at

21   the Xba1 and Kpn1 sites in the pHS723 binary vector that also constitutively express the GUS

22   reporter gene (Nair et al., 2000). The 35S:*RGO*:pHS723 plasmid was transformed into *A.*

23   *tumefaciens* as described in the previous section. Primary transgenic plants were selected on MS

24   agar plates in the presence of 50 μg/ml kanamycin and highly expressing transgenic plants were

25   further confirmed by GUS staining. *B. napus* cv Westar transformation with the 35S:*RGO*:pHS723

26   construct was carried out as previously described (Savitch et al., 2005).

27

28   **Construction of artificial microRNA (amiR) to silence *RGO***

29

30   Artificial microRNA (amiRNA) gene silencing has been efficiently characterized in *Arabidopsis*

31   (Ossowski et al., 2008). The detail of primer designing and step wise procedure for generating

32   amiRNA constructs can be found in Web MicroRNA Designer (http://wmd3.weigelworld.org).

[Type text]

1   The Web MicroRNA Designer was used to generate a 21mer amiRNA
2   (TAACGGAATACACGGTTGCGG) sequence found within the CDS of *RGO* between 68-84 bp
3   to silence *RGO*. Based on this 21mer amiRNA sequence, four primers: [I: microRNA forward (I
4   miR-S68), II: microRNA reverse (II miR-A68), III: microRNA* forward (III miR* S68), IV:
5   microRNA* reverse (IV mir*A68)] were used to engineer the 21mer amiRNA by site-directed
6   mutagenesis into the Arabidopsis endogenous plant microRNA, miR319a. The engineered
7   miRNA319a targets the *RGO* gene for silencing. The following steps were used to engineer the
8   amiRNA and amiRNA* sequences into an endogenous miR319a precursor. First, three PCR
9   fragments using the pRS300 plasmid as template that harbour the miRNA19a were generated. The
10   first PCR amplified a 271 bp fragment with pRS300 A plus IV mir*A68 primer set that generated
11   overlap with one end of the pRS300 plasmid and mir*A68. The second PCR amplified a 170 bp
12   product with III miR* S68 plus II miR-A68 primer set that generated overlap with mir*A68 and
13   miR-A68. The third PCR amplified a 290 bp product with I miR-S68 plus pRS300 B primer set
14   that generated overlap with miR-A68 and other end of pRS300 plasmid. Finally, an overlap PCR
15   was performed using the above three PCR fragments as templates with pRS300 A plus pRS300 B
16   primer set that generated a 699 bp fragment of engineered miRNA19a with overlap of pRS300
17   destined for subsequent cloning. The engineered miRNA19a was cloned into pJET1.2 (Thermo
18   Fisher Scientific, Waltham, MA, USA) and verified by sequencing (Eurofins Genomics,
19   Louisville, KY, USA). The engineered miRNA19a was excised from pJET1.2 with BamH1 and
20   EcoR1, and ligated into the binary vector pBAR1 under the CaMV 35S promoter
21   (35S:amiRNA19a:pBAR1). The construct was transformed to Arabidopsis WT plants via *A.*
22   *tumefaciens* as described in the previous section. Basta-resistant transformed plants on soil were
23   selected using Glufosinate ammonium (AgrEvo). Plants with most reduction of *RGO* transcripts
24   were chosen as silenced lines.

25

26   **Semi-quantitative RT-PCR and quantitative RT-PCR (qPCR)**

27

28   Total RNA were isolated from rosette leaves, cauline leaves, stem and internode, and inflorescence
29   apex tissues six-week old Arabidopsis WT plants grown under long-day conditions using Trizol
30   reagent (Ambion, Thermo Fisher Scientific, Waltham, MA, USA). Total RNA from two-week old
31   roots was isolated using RNAqueous® according to the manufacturer's instructions (Ambion,
32   Thermo Fisher Scientific, Waltham, MA, USA). Total RNA from young and mature siliques were

[Type text]

1   isolated using a method described earlier (Murmu et al., 2010). RNA samples were treated with

2   TURBO DNase™ (Ambion) prior to cDNA synthesis. Total cDNA from each RNA sample was

3   synthesized from 2 µg of RNA template in a 20 µl reaction using Multiscribe reverse transcriptase

4   (Applied Biosystems, Burlington, ON, Canada). The synthesized cDNA samples were diluted 1:5

5   with diethylpyrocarbonate (DEPC)-treated water (Ambion). Semi-quantitative RT-PCR was

6   performed using 2 µl of diluted cDNA as template and gene-specific primers (Supplemental Table

7   S3). Similarly, quantitative RT-PCR (qPCR) reactions were performed using 2 µl of diluted cDNA

8   as the template and gene-specific primers in triplicate by Power SYBR Green Kit and in a StepOne

9   Plus Real-Time PCR System according to manufacturer's instructions (Applied Biosystems) as

10   described earlier (Murmu et al., 2014). For absolute quantification of *RGO* transcripts in different

11   tissues by qPCR, a standard curve method was used where the *RGO* standard curve was created

12   using the *RGO*:pENTR-D-Topo plasmid, and *RGO* transcripts were calculated accordingly.

13   Comparative C_T ($\Delta\Delta C_T$) was used for relative quantification of transcripts of *GLK1* with GLK1-

14   F2 plus GLK1-R2 primer set; and *RGO* with RGO-QF3 plus RGO-QR3 primer set and normalized

15   using two endogenous control genes, *eIF4A-1* (*At3g13920*), and *GAPC* (*At3g04120*). The data

16   represents three biological replicates with three technical replicates of each. All the qPCR data

17   were analysed with $P < 0.05$ as statistically significant value using the StepOne 2.1 software

18   (Applied Biosystems). A list of the genes and primers used in RT-PCR and qPCR is found in

19   Supplemental Table S2.

20

21   **Green callus formation assay**

22

23   Surface sterilized and stratified seeds were grown in square petri dish (VWR International, Ltd,

24   Quebec, Canada) on half MS salt plus 0.7 % (w/v) Agar plates in the dark at room temperature

25   for five days. After five days, root portion was excised out with a razor blade in a sterile laminar

26   flow hood and immediately transferred onto half MS plus agar plate supplemented with 0.005

27   µM 2,4-D (2,4-Dichlorophenoxyacetic acid), a synthetic auxin, plus varying concentrations

28   (0.005 to 0.5 µM) of BA (6-Benzylaminopurine) according to a procedure described earlier (Kiba

29   et al., 2005). Plates were grown for an additional 30 days under long-day photoperiod conditions

30   for generation of green calli. Green calli images were photographed with a Nikon D90 DSRL.

31

32   **Root growth assays**

[Type text]

1

2 Sterilized seeds were placed on square petri plates (VWR International, Ltd, Quebec, Canada)

3 containing minimal agar media (Haughn and Somerville, 1986) alone or supplemented either with

4 1% sucrose or 5 μm Kinetin (a synthetic CK). Plates were sealed with two layers of parafilm and

5 grown vertically under a long-day growth cabinet for seven-day. At least 10 seeds from each

6 genotype were placed on each plate with five to six replicates of the plates. The root growth assay

7 was repeated three times with similar results. Roots were photographed with a Nikon D90 DSRL

8 camera and root lengths were measured from the digital photographs with ImageJ software

9 (https://imagej.nih.gov/ij/).

10

11 **Subcellular localization studies**

12

13 For subcellular localization, leaf discs were prepared from three-week old soil grown Arabidopsis

14 plants and stained for 1 hour with 10 μM DAPI (4',6-Diamidino-2-Phenylindole, Dihydrochloride)

15 in the dark at room temperature. After 1 hour the leaf discs were washed three times with sterile

16 water and then mounted in Fluoromount-G ^{TM} (Electron microscopy Sciences, Hatfield, PA, USA).

17 Leaf discs were imaged with a Zeiss LSM800 Airyscan laser scanning confocal microscope (Carl

18 Zeiss MicroImaging, Göttingen, Germany). For visualisation of DAPI and YFP, excitation lasers

19 at 405 nm, 488 nm respectively were used and emission was monitored between 400 nm to 580

20 nm, 490 nm to 585 nm were acquired using the GaAsP detector and a Plan-Apochromat 63X/1.46

21 objective lens. For plasma membrane visualisation, leaf discs were stained with the lipophilic styryl

22 fluorescent dye FM4-64FX (Molecular Probes, Eugene, OR, USA) at a concentration of 0.01

23 μg/mL in 1xPBS (Phosphate buffer saline) pH 7.4 and were incubated for 2 hours at room

24 temperature in the dark. Subsequently, leaf discs were mounted in fresh dye and imaged with a

25 Plan-Apochromat 63x/1.4 objective lens and the high resolution Airyscan detector using excitation

26 laser line 488 nm and emission bands 490 nm to 580 nm, and 635 nm to 700 nm for YFP and

27 plasma membrane, respectively. For endoplasmic reticulum (ER) localization of 35S:*GFP:HDEL*,

28 an ER marker (Batoko et al., 2000) and 35S:*RGO:YFP* were infiltrated into four-week old

29 *Nicotiana benthamiana* leaves via *Agrobacterium tumefaciens* according to a procedure previously

30 described (Kosma et al., 2014). GFP and YFP fluorescence was monitored three days post

31 infiltration. Essentially, leaf discs were mounted in Fluoromount-G ^{TM} and YFP fluorescence was

32 captured as described above. Similarly, GFP fluorescence was detected with excitation laser 488

[Type text]

1 nm and emission was monitored between 490 nm to 585 nm using the GaAsP detector and a Plan-

2 Apochromat 63X/1.46 objective lens. For ER localization, similar plane and cell-types were

3 imaged. All the confocal images were processed with ZEN 2.1 (Zeiss MicroImaging, Göttingen,

4 Germany) and Adobe Photoshop CS6 (http://www.adobe.com/).

5

6 **Chlorophyll retention of dark-induced senescence with BA (6-Benzylaminopurine)**

7 **treatment**

8

9 Rosette leaves number 4 and 5 from four-week old plants of WT, 35S:*RGO*, and *rgo* plants grown

10 in a long-day photoperiod conditions were used for this assay. Two set of six leaves from each

11 genotypes were floated in a volume of 20 ml sterile water with 0.01N NaOH (-BA) or with 5 μM

12 BA in 0.01N NaOH (+BA) in a petri dish, wrapped with aluminum foil and incubated in dark for

13 seven days according to a procedure described earlier (Vercruyssen et al., 2015). After seven days

14 of dark treatments (-BA, +BA), the leaves were imaged with a Nikon D90 digital SLR camera. The

15 second set of leaves with similar treatments were used for chlorophyll (Chl: Chl a + Chl b)

16 measurements. Two of 0.5 cm^2 leaf disc were resuspended in 1ml DMF *(N,N*-Dimethylformamide)

17 in the dark at 4^0 C overnight for total Chl extraction and Chl was measured with UV-visible

18 spectrophotometer (Thermo Scientific) at 647 nm and 664.5 nm in 1 mm cuvettes. Total Chl was

19 calculated per cm^2 according to a procedure described earlier (Inskeep and Bloom, 1985). The

20 experiment was repeated three times.

26

27 **LITERATURE CITED**

28

[Type text]

1 Ashikari M, Sakakibara H, Lin S, Yamamoto T, Takashi T, Nishimura A, Angeles ER, Qian Q,
2   Kitano H, Matsuoka M (2005) Cytokinin oxidase regulates rice grain production. Science 309:
3   741-745

4 Balasubramanian B, Lowry CV, Zitomer RS (1993) The Rox1 repressor of the Saccharomyces
5   cerevisiae hypoxic genes is a specific DNA-binding protein with a high-mobility-group motif.
6   Mol Cell Biol 13: 6071-6078

7 Bartrina I, Otto E, Strnad M, Werner T, Schmülling T (2011) Cytokinin regulates the activity of
8   reproductive meristems, flower organ size, ovule formation, and thus seed yield in Arabidopsis
9   thaliana. Plant Cell 23: 69-80

10 Batoko H, Zheng HQ, Hawes C, Moore I (2000) A Rab1GTPase is required for transport between
11   the endoplasmic reticulum and Golgi apparatus and for normal Golgi movement in plants. Plant
12   Cell 12: 2201-2218

13 Caesar K, Thamm AMK, Witthöft J, Elgass K, Huppenberger P, Grefen C, Horak J, Harter K
14   (2011) Evidence for the localization of the Arabidopsis cytokinin receptors AHK3 and AHK4
15   in the endoplasmic reticulum. J Exp Bot 62: 5571-5580

16 Clough SJ, Bent AF (1998) Floral dip: a simplified method for agrobacterium-mediated
17   transformation of Arabidopsis thaliana. Plant J 16: 735-743

18 Cortleven A, Marg I, Yamburenko MV, Schlicke H, Hill K, Grimm B, Schaller GE, Schmülling T
19   (2016) Cytokinin regulates the etioplast-chloroplast transition through the two-component
20   signaling system and activation of chloroplast-related genes. Plant Physiol 172: 464-478

21 Cortleven A, Schmülling T (2015) Regulation of chloroplast development and function by
22   cytokinin. J Exp Bot 66: 4999-5013

23 Curtis MD, Grossniklaus U (2003) A gateway cloning vector set for high-throughput functional
24   analysis of genes in planta. Plant Physiol 133: 462-469

25 Deckert J, Rodriguez Torres AM, Simon JT, Zitomer RS (1995) Mutational analysis of Rox1, a
26   DNA-bending repressor of hypoxic genes in Saccharomyces cerevisiae. Mol Cell Biol 15:
27   6109-6117

28 Fitter DW, Martin DJ, Copley MJ, Scotland RW, Langdale JA (2002) GLK gene pairs regulate
29   chloroplast development in diverse plants. Plant J 31:713-727

30 Gan S, Amasino RM (1995) Inhibition of leaf senescence by auto- regulated production of
31   cytokinin. Science 270: 1986-1988

[Type text]

Garapati P, Xue G-P, Munné-Bosch A, Balazadeh S (2015) Transcription factor ATAF1 in Arabidopsis promotes senescence by direct regulation of key chloroplast maintenance and senescence transcriptional cascades. Plant Physiol 168: 1122-1139

Goda H, Sasaki E, Akiyama K, Maruyama-Nakashita, Nakayabashi K, Li W, Ogawa, M, Yamaguchi Y, Preston J, Aoiki K et al., (2008) The ATGenExpress hormone and chemical treatment data set: experimental design, data evaluation, model data analysis and data access. Plant J 55: 526-542

Guan P, Ripoll JJ, Wang R, Vuong L, Bailey-Steinitz LJ, Ye D, Crawford NM (2017) Interacting TCP and NLP transcription factors control plant responses to nitrate availability. Proc Natl Acad Sci USA 114: 2419-2424

Guo L, Han A, Bates DL, Cao J, Chen L (2007) Crystal structure of a conserved N-terminal domain of histone deacetylase 4 reveals functional insights into glutamine-rich domains. Proc Natl Acad Sci USA 104: 4297-4302

Häffner E, Konietzki S, Diederichsen E (2015) Keeping Control: The Role of Senescence and Development in Plant Pathogenesis and Defense. Plants (Basel) 4: 449-488.

Haughn GH, Somerville C (1986) Sulfonylurea-resistant mutants of Arabidopsis thaliana. Mol Gen Genet 204: 430-434

Hill K, Mathews DE, Kim HJ, Street IH, Wildes SL, Chiang YH, Mason MG, Alonso JM, Ecker JR, Kieber JJ, Schaller GE (2013) Functional characterization of type-B response regulators in the Arabidopsis cytokinin response. Plant Physiol 162: 212-224

Howell SH, Lall S, Che P (2003) Cytokinins and shoot development. Trends Plant Sci 8: 453-459

Inskeep WP, Bloom PR (1985) Extinction coefficients of chlorophyll a and B in N,N-dimethylformamide and 80% acetone. Plant Physiol 77: 483-485

Kiba T, Naitou T, Koizumi N, Yamashino T, Sakakibara H, Mizuno T (2005) Combinatorial microarray analysis revealing Arabidopsis genes implicated in cytokinin responses through the His-Asp phosphorelay circuitry. Plant Cell Physiol 46: 339-355

Kieber JJ, Schaller GE (2014) Cytokinins. The Arabidopsis Book e0168

Kim HJ, Ryu H, Hong SH, Woo HR, Lim PO, Lee IC, Sheen J, Nam HG, Hwang I (2006) Cytokinin-mediated control of leaf longevity by AHK3 through phosphorylation of ARR2 in Arabidopsis. Pro Natl Acad Sci USA 103: 814-819

[Type text]

Kobayashi K, Baba S, Obayashi T, Sato M, Toyooka K, Keränen M, Aro EM, Fukaki H, Ohta H, Sugimoto K, Masuda T (2012) Regulation of root greening by light and auxin/cytokinin signaling in Arabidopsis. Plant Cell 24: 1081-1095

Kobayashi K, Ohnishi A, Sasaki D, Fujii S, Iwase A, Sugimoto K, Masuda T, Wada H (2017) Shoot removal induces chloroplast development in roots via cytokinin signaling. Plant Physiol 173: 2340-2355

Kosma DK, Murmu J, Razeq FM, Santos P, Bourgault R, Molina I, Rowland O (2014) AtMYB41 activates ectopic suberin synthesis and assembly in multiple plant species and cell types. Plant J 80: 216-229

Kuiper EFE, de Mattos EP, Jardim LB, Kampinga HH, Bergink S (2017) Chaperones in polyglutamine aggregation: Beyond the Q-stretch. Front Neurosci 11: 145

Lai Z, Wang F, Zheng Z, Fan B, Chen Z (2011) A critical role of autophagy in plant resistance to necrotrophic fungal pathogens. Plant J 66: 953-968

Lewis LA, Polanski K, de Torres-Zabala M, Jayaraman S, Bowden L, Moore J, et al (2015) Transcriptional dynamics driving MAMP-triggered immunity and pathogen effector-mediated immunosuppression in Arabidopsis leaves following infection with Pseudomonas syringae pv tomato DC3000. Plant Cell 27: 3038-3064

Lin YJ, Cao ML, Xu CG, Chen H, Wei J, Zhang QF (2002) Cultivating rice with delaying led-senescence by P-SAG12-IPT gene transformation. Act Bot Sin 44: 1333-1338

Liu YD, Yin ZJ, Yu JW, Li J, Wei HL, Han XL, Shen FF (2012) Improved salt tolerance and delayed leaf senescence in transgenic cotton expressing the Agrobacterium IPT gene. Biol Plant 56: 237-246

Lomin SN, Myakushina YA, Arkhipov DV, Leonova OG,,Popenko VI, Schmülling T, Romanov GA (2018) Studies of cytokinin receptor-phosphotransmitter interaction provide evidences for the initiation of cytokinin signalling in the endoplasmic reticulum. Funct Plant Biol 45: 192-202

Lomin SN, Yonekura-Sakakibara K, Romanov GA, Sakakibara H (2011) Ligand-binding properties and subcellular localization of maize cytokinin receptors. J Exp Bot 62: 5149-5159

Lupi ACD, Lira BS, Gramegna G, Trench B, Alves FRR, Demarco D, Peres LEP, Purgatto E, Freschi L, Rossi M (2019) Solanum lycopersicum GOLDEN 2-LIKE 2 transcription factor affects fruit quality in a light- and auxin-dependent manner. PLoS One 14: e0212224

[Type text]

Ma QH, Liu YC (2009) Expression of isopentenyl transferase gene (*ipt*) in leaf and stem delayed leaf senescence without affecting root growth. Plant Cell Rep 28: 1759-1765

Martín G, Leivar P, Ludevid D, Tepperman JM, Quail PH, Monte E (2016) Phytochrome and retrograde signalling pathways converge to antagonistically regulate a light-induced transcriptional network. Nat Commun 7: 11431

Miyawaki K, Tarkowski P, Matsumoto-Kitano M, Kato T, Sato S, Tarkowska D, Tabata S, Sandberg G, Kakimoto T (2006) Roles of Arabidopsis ATP/ADP isopentenyltransferases and tRNA isopentenyltransferases in cytokinin biosynthesis. Pro Natl Acad Sci USA 103: 16598-16603

Mok DW, Mok MC (2001) Cytokinin metabolism and action. Annu Rev Plant Physiol Plant Mol Biol 52: 89-118

Murmu J, Bush MJ, DeLong C, Li S, Xu M, Khan M, Malcolmson C, Fobert PR, Zachgo S, Hepworth SR (2010) Arabidopsis basic leucine-zipper transcription factors TGA9 and TGA10 interact with floral glutaredoxins ROXY1 and ROXY2 and are redundantly required for anther development. Plant Physiol 154: 1492-1504

Murmu J, Wilton M, Allard G, Pandeya R, Desveaux D, Singh J, Subramaniam R (2014) Arabidopsis Golden2-like transcription factors (GLK) activate JA-dependent disease susceptibility against the biotrophic pathogen Hyaloperonospora arabidopsidis as well as JA-independent plant immunity against the necrotrophic pathogen Botrytis cinerea. Mol Plant Pathol 15: 174-184

Muthuramalingam M, Wang Y, Li Y, Mahalingam R (2017) Interacting protein partners of Arabidopsis RNA-binding protein AtRBP45b. Plant Biol (Stuttg) 19: 327-334

Nair RB, Joy RW[4th], Kurylo E, Shi X, Schnaider J, Datla RS, Keller WA, Selvaraj G (2000) Identification of a CYP84 family of cytochrome P450-dependent mono-oxygenase genes in Brassica napus and perturbation of their expression for engineering sinapine reduction in the seeds. Plant Physiol 123: 1623-1634

Nelson BK, Cai X, Nebenführ A (2007) A multicolored set of in vivo organelle markers for co-localization studies in Arabidopsis and other plants. Plant J 51: 1126-1136

Ossowski S, Schwab R, Weigel D (2008) Gene silencing in plants using artificial microRNAs and other small RNAs. Plant J 53:674-690

Perutz MF, Johnson T, Suzuki M, Finch JT (1994) Glutamine repeats as polar zippers: their possible role in inherited neurodegenerative diseases. Proc Natl Acad Sci USA 91: 5355-5358

[Type text]

1 Raines T, Shanks C, Cheng CY, McPherson D, Argueso CT, Kim HJ, Franco-Zorrilla JM, López-Vidriero I, Solano R, Vaňková R, Schaller GE, Kieber JJ (2016) The cytokinin response factors modulate root and shoot growth and promote leaf senescence in Arabidopsis. Plant J 85: 134-147

Rauf M, Arif M, Dortay H, Matallana-Ramírez LP, Waters MT, Gil Nam H, Lim PO, Mueller-Roeber B, Balazadeh S (2013) ORE1 balances leaf senescence against maintenance by antagonizing G2-like-mediated transcription. EMBO Rep 14: 382-388

Reichmann JL, Heard J, Martin G, Reuber L, Jiang CZ, Keddie J, Adam L, Pineda O, Ratcliffe OJ, Samaha RR, Creelman R, Pilgrim M, Broun P, Zhang JZ, Ghandehari D, Sherman BK, Yu GL (2000) Arabidopsis transcription factors: genome-wide comparative analysis among eukaryotes. Science 290: 2105-2110

Richmond AE, Lang A (1957) Effect of kinetin on protein content and survival of detached Xanthium leaves. Science 125: 650-651

Romanov GA, Lomin SN, Schmülling T (2018) Cytokinin signaling: from the ER or from the PM? That is the question! New Phytol 218: 41-53

Savitch LV, Allard G, Seki M, Robert LS, Tinker NA, Huner NP, Shinozaki K, Singh J (2005) The effect of overexpression of two Brassica CBF/DREB1-like transcription factors on photosynthetic capacity and freezing tolerance in Brassica napus. Plant Cell Physiol 46: 1525-1539

Savitch LV, Subramaniam R, Allard G, Singh J (2007) The GLK1 'regulon' encodes disease defense related proteins and confers resistance to Fusarium graminearum in Arabidopsis. Biochem Biophys Res Commun 359: 234-238

Skoog F, Miller CO (1957) Chemical regulation of growth and organ formation in plant tissue cultured. In Vitro Symp Soc Exp Biol 11: 118-131

Schmülling T, Werner T, Riefler M, Krupkov E, Bartrina y Manns I (2003) Structure and function of cytokinin oxidase/dehydrogenase genes of maize, rice, Arabidopsis and other species. J Plant Res 116: 241-252

Swartzberg D, Kirshner B, Rav-David D, Elad Y, Granot D (2008) Botrytis cinerea induces senescence and is inhibited by autoregulated expression of the *IPT* gene. Eur J Plant Pathol 120: 289-297

31

[Type text]

1 TajimaY, Imamura A, Kiba T, Amano Y, Yamashino T, Mizuno T (2004) Comparative studies on the type-B response regulators revealing their distinctive properties in the His-to-Asp phosphorelay signal transduction of Arabidopsis thaliana. Plant Cell Physiol 45: 28-39

Talla SK , Panigrahy M, Kappara S, Nirosha P, Neelamraju S, Ramanan R (2016) Cytokinin delays dark-induced senescence in rice by maintaining the chlorophyll cycle and photosynthetic complexes. J Exp Bot 67: 1839-1851

Thatcher LF, Kamphuis LG, Hane JK, Oñate-Sánchez L, Singh KB (2015) The Arabidopsis KH-domain RNA-binding protein ESR1 functions in components of jasmonate signalling, unlinking growth restraint and resistance to stress. PLoS One 10: e0126978

Tokumaru M, Adachi F, Toda M, Ito-Inaba Y, Yazu F, Hirosawa Y,Sakakibara Y, Suiko M, Kakizaki T, Inaba T (2017) Ubiquitin-proteasome dependent regulation of the GOLDEN2 LIKE 1 transcription factor in response to plastid signals. Plant Physiol 173: 524–535

Vercruyssen L, Tognetti VB, Gonzalez N, Van Dingenen J, De Milde L, Bielach A, De Rycke R, Van Breusegem F, Inzé D (2015) GROWTH REGULATING FACTOR5 stimulates Arabidopsis chloroplast division, photosynthesis, and leaf longevity. Plant Physiol 167: 817-832

Wang H, Liu G, Li C, Powell AL, Reid MS, Zhang Z, Jiang CZ (2013) Defence responses regulated by jasmonate and delayed senescence caused by ethylene receptor mutation contribute to the tolerance of petunia to Botrytis cinerea. Mol Plant Pathol 14: 453-469

Waters MT, Moylan EC, Langdale JA (2008) GLK transcription factors regulate chloroplast development in a cell-autonomous manner. Plant J 56: 432-444

Waters MT, Wang P, Korkaric M, Capper RG, Saunders NJ, Langddale JA (2009) GLK transcription factors coordinate expression of the photosynthetic apparatus in Arabidopsis. Plant Cell 21: 1109-1128

Werner T, Motyka V, Strnad M, Schmülling T (2001) Regulation of plant growth by cytokinin. Proc Natl Acad Sci USA 98: 10487-10492

Werner T, Motyka V, Laucou V, Smets R, Van Onckelen H, Schmülling T (2003) Cytokinin-deficient transgenic Arabidopsis plants show multiple developmental alterations indicating opposite functions of cytokinins in the regulation of shoot and root meristem activity. Plant Cell 15: 2532-2550

Werner T, Schmülling T (2009) Cytokinin action in plant development. Curr Opin Plant Biol 12: 527-538

[Type text]

1 Wu Y, Gong W, Yang W (2017) Shade Inhibits Leaf Size by Controlling Cell Proliferation
2   and Enlargement in Soybean. Sci Rep 7: 9259

3

4 Wulfetange K, Lomin SN, Romanov GA, Stolz A, Heyl A, Schmülling T (2011) The cytokinin
5   receptors of Arabidopsis are located mainly to the endoplasmic reticulum. Plant Physiol 156:
6   1808-1818
7 Yang C, Li L (2017) Hormonal Regulation in Shade Avoidance. Front Plant Sci 8: 1527.
8 Yasumura Y, Moylan EC, Langdale JA (2005) A conserved transcription factor mediates nuclear
9   control of organelle biogenesis in anciently diverged land plants. Plant Cell 17: 1894-1897
10 Yeh SY, Chen HW, Ng CY, Lin CY, Tseng TH, Li WH, Ku MS (2015) Down-regulation of
11   cytokinin oxidase 2 expression increases tiller number and improves rice yield. Rice 8: 36
12 Zalewski W, Galuszka P, Gasparis S, Orczyk W, Nadolska-Orczyk A (2010) Silencing of the
13   HvCKX1 gene decreases the cytokinin oxidase/dehydrogenase level in barley and leads to
14   higher plant productivity. J Exp Bot 61: 1839-1851
15 Zalewski W, Gasparis S, Boczkowska M, Rajchel IK, Kała M, Orczyk W, Nadolska-Orczyk A
16   (2014) Expression patterns of HvCKX genes indicate their role in growth and reproductive
17   development of barley. PLoS One 9: e115729
18 Zalewski W, Orczyk W, Gasparis S, Nadolska-Orczyk A (2012) HvCKX2 gene silencing by
19   biolistic or Agrobacterium-mediated transformation in barley leads to different phenotypes.
20   BMC Plant Biol 12: 206
21 Zhang L, Zhao YL, Gao LF, Zhao GY, Zhou RH, Zhang BS, Jia JZ (2012) TaCKX6-D1, the
22   ortholog of rice OsCKX2, is associated with grain weight in hexaploid wheat. New Phytol 195:
23   574-584
24 Zhang P, Wang WQ, Zhang GL, Kaminek M, Dobrev P, Xu J, Gruissem W (2010) Senescence-
25   inducible expression of isopentenyl transferase extends leaf life, increases drought stress
26   resistance and alters cytokinin metabolism in cassava. J Integr Plant Biol 52: 653-669

27

28 **FIGURE LEGENDS**

29

30 **Figure 1**

31 **Deduced amino acid sequence and upregulation of *Arabidopsis Response to GLK1***

32 **_Overexpression_ (*RGO, At1g77960*).** (A) amino acid sequence of *At*RGO in single-letter code and

[Type text]

1   the glutamine rich region is highlighted in gray. Numbering of amino acids are on the right. (B)

2   Transcripts accumulation of *AtGLK1* and *AtRGO* in wild-type (WT), *glk1* mutant, and

3   35S:*AtGLK1* plants with RT-PCR compared to *eIF4A-1*, a housekeeping gene transcripts; (C)

4   *AtGLK1* and *AtRGO* transcripts with qPCR relative to *eIF4A-1* and *GAPC,* two housekeeping gene

5   transcripts. Relative transcripts represent as mean fold change values ± standard error of mean

6   (SEM) from three biological replicates.

7

8   **Figure 2**

9   **Expression pattern of *AtRGO*.** (A) *AtRGO* transcripts accumulation in wild-type (WT) Col-0

10   with RT-PCR compared to *eIF4A-1* and *GAPC,* two housekeeping control transcripts; (B)

11   Absolute quantification of *AtRGO* transcripts with qPCR. Transcripts represented are mean fold

12   change values ± standard error of mean (SEM) from three biological replicates; (C) *AtRGO*

13   promoter driven reporter GUS reporter gene expression in WT plants. GUS expression was

14   observed starting one day after germination; GUS expression was intense in cotyledons and

15   slowly progressed to vascular tissues in the root. Scale bar, 200 μm in seedlings, and bar, 1 cm in

16   mature tissues.

17

18   **Fig. 3**

19   **Subcellular localization of *At*RGO-YFP fusion protein by confocal microscopy in transgenic**

20   **Arabidopsis leaves and tobacco leaves.** Plants expressing 35S:YFP were used as positive control

21   (A-C) for comparing *At*RGO-YFP fusion expression (D-F). (A and D), YFP signal in yellow; (B

22   and E), DAPI strained nuclei in blue; (C and F) merged. Arrow head shows the nucleus and

23   endoplasmic reticulum (ER). Zoom in view of 35S:YFP (G) and *At*RGO:YFP (H) with FM4-64FX

24   stain. YFP fluorescence in yellow and plasma membrane stain in blue, a false colour for contrast

25   is shown in G-H and arrow head shows the nucleus and plasma membrane (PM) in G-H. Transient

26   expression of *At*RGO-YFP (I) and GFP:HDEL, an ER marker (J) in tobacco leaves. Arrow head

27   shows the ER in I-J. Scale bar, 20 μm in A-F and 5 μm in G-J.

28

29   **Figure 4**

30   **Phenotype of *rgo* plants compared to WT (Col-0).** (A) A RT-PCR of full length *AtRGO*

31   transcripts in WT and *rgo* plants compared to *eIF4A-1* and *GAPC* transcripts; (B) qPCR of

34

[Type text]

1   *AtRGO* transcripts in WT and *rgo* plants; (C) phenotype at four-week age; (D) phenotype at six-

2   week age. Scale bar, 1 cm in C-D.

3

4   **Figure 5**

5   **Root growth phenotype of WT, *rgo* and *35S: AtRGO* lines at seven days post germination.**

6   (A) representative images on minimal media (MM), (B) corresponding root length. Error bar =

7   standard error of mean. Scale bar, 1 cm in A. Statistical significance of root lengths were

8   analyzed using student's t-test: Two sample assuming unequal variance at 95% confidence level.

9   *** represents the p value < 0.00000001, and * represents p value > 0.1.

10

11   **Figure 6**

12   **Phenotype of *35S:AtRGO* plants compared to WT.** (A) A RT-PCR of full length *AtRGO*

13   transcripts compared to *eIF4A-1* and *GAPC* transcripts in WT and three independent lines of

14   *35S:AtRGO* plants; (B) qPCR of *AtRGO* transcripts in WT and *AtRGO* overexpressing lines; (C)

15   Four-week old plants; (D) Five-week old plants. Emergence of inflorescence buds are shown

16   with arrow head in C and axillary buds in D; (E) Average seed yield from 10 Arabidopsis plants

17   of WT and *35S:AtRGO* from a long-day photoperiod growth conditions; (F) seed yield from

18   individual plants of *B. napus* in WT and *35S:AtRGO* (two lines). Scale bar, 1cm in C-D.

19   Statistical significance was analysed using student's t-test: Two-sample assuming unequal

20   variances at 95% confidence level compared with empty vector. The p value for each analysis is

21   shown as asterisk, where p value ≤ 0.001 (**). Error bar = standard error of mean.

22

23   **Figure 7**

24   **Cytokinin (CK) response, CK levels in 35S:*AtRGO* and *rgo* silenced plants.** (A)

25   Hypersensitive response of *35S:AtGLK1* plants to BA, a synthetic cytokinin (CK), in green calli

26   formation. WT and *35S:AtGLK1* seeds were germinated in dark for five days on half strength MS

27   agar plates then elongated hypocotyls were excised out and grown on half strength MS agar

28   plates supplemented with 0.005 μM 2,4-D plus varying concentration (0.005 to 1 μM) of BA

29   under long-day photoperiod conditions. After 30 days representative callus were photographed.

30   Scale bar = 1 cm. (B) Root length of seedlings at seven days post germination on minimal agar

31   media in absence or presence of 5 μM CK, *represents the p value < 0.001; (C) Green callus

32   formation from excised hypocotyl in presence of 0.005 μM 2,4-D plus 0.5 μM BA (CK) on MS

35

[Type text]

1   agar plates of WT, 35S:*AtRGO* and *rgo*. Scale bar = 1 cm. (D) Effect of exogenous application of

2   CK on leaf chlorophyll (Chl) retention during dark-induced senescence; (E) Bioactive CK [zeatin

3   (tZ, open bar) and 2-isopentenyladenine (2iP, grey bar)] level in four-week old rosette leaves. p

4   value < 0.001 (**) and p value <0.01 (*). Error bars = SE (n=3). * denotes the significant

5   difference between –BA and +BA treatment (p<0.001, Student's t-test); (F) Relative transcripts

6   of *CKX4* and *CKX5* quantified with qPCR in four week old leaves of wild-type (WT) Col-0,

7   35S:*AtRGO*, and *rgo,* compared to *eIF4A-1* and *GAPC,* two housekeeping control transcripts.

8   Relative transcripts (RQ) represent as mean fold change values ± standard error of mean (SEM)

9   from three biological replicates. Error bars = SE (n=3). * denotes the statistical significant

10   (p<0.001, Student's t-test).

11

12

13

14
15
16
17
18
19
20